Lawrence Berkeley National Laboratory

Title
Elastic Scattering of 190 MEV Deuterons by Protons

Permalink
https://escholarship.org/uc/item/3p71b2vf

Authors
Chamberlain, Owen
Stern, Martin O.

Publication Date
1953-06-03

UNIVERSITY OF CALIFORNIA

Radiation Laboratory

Contract No. W-7405-eng-48

ELASTIC SCATTERING OF 190 MEV DEUTERONS BY PROTONS

Owen Chamberlain and Martin O. Stern

June 3, 1953

Berkeley, California

ELASTIC SCATTERING OF 190 MEV DEUTERONS BY PROTONS

Owen Chamberlain and Martin O. Stern

Radiation Laboratory, Department of Physics
University of California, Berkeley, California

June 3, 1953

ABSTRACT

The elastic differential scattering cross section of 190 Mev deuterons by protons has been measured from 15° to 170° in the center of mass system. The cross sections were obtained by subtracting the carbon counts from those received with a polyethylene target. Part I presents a description of the experiments. Results are shown in Table IV and Fig. 3. Part II compares these results with those expected from theory by making use of a method developed by Chew.[1] A summary of this comparison is given in Table VII.

ELASTIC SCATTERING OF 190 MEV DEUTERONS BY PROTONS

Owen Chamberlain and Martin O. Stern[+]

Radiation Laboratory, Department of Physics
University of California, Berkeley, California

June 3, 1953

INTRODUCTION

In the preceding paper[2] it was stated that because of the interference between n-p and p-p scattering in d-p scattering the latter might provide information on nucleon-nucleon scattering that n-p and p-p experiments alone could not reveal. In this respect elastic d-p scattering, because of the single final deuteron state involved, exhibits the largest amount of interference, and, being theoretically somewhat amenable, offers, at this time at least, one of the ways to obtain more information about nuclear forces.

This paper is divided into two parts. Part I describes the experiment. Since the apparatus was almost the same as that used in the inelastic and total scattering experiments, it will not be described in detail except where different from that of BC. Part II attempts to compare experimental results with theory.

I EXPERIMENT

A. Method and Procedure.

Source of particles, targets, method of detection, and monitoring device have been described in BC.

Four methods of operation were used. In method A, the pulses from the distributed amplifiers went directly to a fast coincidence circuit[3] whose output fed into a scaler. Methods B, C, and D made use of a pulse shaper-discriminator designed by A. L. Bloom. In method B (cf. Fig. 1, BC), two crystals were used, one on each arm of the scattering table, and their single counts and coincidences were recorded. Method C was of value whenever one arm had to be placed at small angles to the beam, where a large background of charged particles was to be expected. Two crystal detectors were placed telescope fashion on this arm, and three single counting rates, as well as their triple coincidence and the double coincidence from the telescope, were recorded. Method D, finally, employed a single detector. All methods agreed within statistical errors in the regions in which results obtained with them overlapped. Furthermore, methods A, B, C were used interchangeably, and we shall not distinguish between them in what follows, but merely group all results under the headings "coincidence method" (A, B, or C) or "single count method" (D).

The experimental procedure used to check circuits and geometry prior to the recording of actual data was identical to that outlined in BC.

B. Kinematics and Geometry.

Let M be the rest mass of a particle incident with kinetic energy E in the laboratory system on another particle of rest mass m, initially at rest. The two particles collide; that of mass M is deflected to a direction Θ, that of mass m, to a direction $\bar{\Phi}$, with respect to the incident beam in the laboratory system. Let θ be the angle of deflection of either particle in the center of mass system. We have then

$$\rho = \frac{m}{M}, \quad \epsilon = \frac{E}{Mc^2}, \quad \beta = \frac{\left[(\epsilon + 1)^2 - 1\right]^{1/2}}{\epsilon + 1 + \rho};$$

$$\gamma = \frac{1}{\left[1 - \beta^2\right]^{1/2}} \quad \text{and} \quad A = \gamma \frac{\epsilon + 1 + 1/\rho}{\epsilon + 1 + \rho},$$

(1)

where β is the ratio of the velocity of the mass m in the center of mass system to that of light.

We can then derive the following relativistic relations:

$$\gamma \tan \frac{\theta}{2} = \cot \bar{\Phi}, \tag{2}$$

$$\tan \bar{\Theta} = \frac{2 \tan \theta/2}{A + \gamma + (A - \gamma) \tan^2 \theta/2}, \tag{3}$$

$$E_m = 2 mc^2 \beta^2 \gamma^2 \sin^2 \theta/2, \tag{4}$$

and

$$E_M = E - E_m, \tag{5}$$

where E_M, E_m are the energies of incident and struck particle in the laboratory after the collision. The energy available in the center of mass system is

$$E_o = E/\gamma - c^2 (m + M)(1 - 1/\gamma) \tag{6}$$

and the initial momentum p_i and final momentum p_f in the center of mass system are

$$p_i = p_{ix} = mc\beta\gamma, \quad p_{fx} = mc\beta\gamma \cos \theta, \quad p_{fy} = mc\beta\gamma \sin \theta, \tag{7}$$

where x and y are directions in the scattering plane along and perpendicular to the beam, respectively.

In our case (Fig. 1) the deuteron is to be identified with M, $\bar{\Theta}$, the proton with m, $\bar{\Phi}$; $\rho \approx 1/2$, $\epsilon = 0.1023$, and $\beta = 0.29$ so that relativistic corrections are slight, although the exact relations were used in the presentation of our results. For purposes of discussion it is sufficient to consider these relations in their non-relativistic limits, $\gamma = 1$ and $A = 1/\rho$. It is then easy to see that:

(1) The center of mass angle θ and the laboratory angle of deflection of the proton $\bar{\Phi}$ are double-valued functions of the laboratory angle of deflection of the deuteron, $\bar{\Theta}$. Thus, when $\bar{\Theta} = 0°$, $\theta = 0°$ or $180°$ and $\bar{\Phi} = 90°$ or $0°$.

(2) $\bar{\Theta} \leqslant 30°$; at $\bar{\Theta} = 30°$, $\bar{\Phi} = 30°$ and $\theta = 120°$.

(3) The energy of the struck proton reaches its maximum of $8/9$ E or about 171 Mev when $\theta = 180°$. In the region $0° \leqslant \theta \leqslant 120°$, $1 \geqslant \frac{E_M}{E} \geqslant 1/3$, and in the region $120° \leqslant \theta \leqslant 180°$, $1/3 \geqslant \frac{E_M}{E} \geqslant 1/9$.

The kinematics of elastic scattering for small and large θ are summarized in Table I.
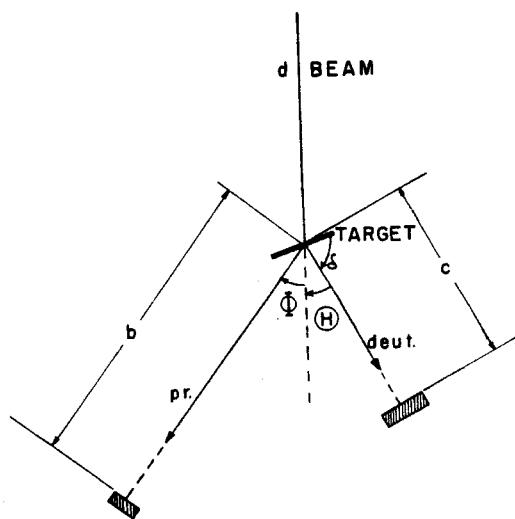
MU-2299A

Fig. 1

TABLE I

Angles and energies of deuterons and protons resulting from elastic scattering of 192 Mev deuterons on hydrogen. Φ and Θ are angles of deflection of proton and deuteron, respectively, in the laboratory system; θ is the angle of deflection in the center of mass system.

Φ degrees	Θ degrees	θ degrees	Proton Energy Mev	Proton Range g/cm² Al[a]	Deuteron Energy Mev	Deuteron Range g/cm² Al[a]	$\dfrac{d\cos\Phi}{d\cos\theta}$	$\dfrac{d\cos\Theta}{d\cos\theta}$
0	0	180	172	25.4	20	0.33	0.229	1.046
5	10.3	169.5	170	25.0	22	0.39	0.230	0.913
10	18.8	159.2	166	24.0	26	0.52	0.234	0.625
15	24.7	148.7	159	22.4	33	0.81	0.240	0.356
65.5	15	47.1	28	1.04	164	14.5	0.639	0.107
73.8	10	31.1	13	0.26	179	16.8	0.966	0.107
82.0	5	15.4	3	0.02	189	18.3	1.956	0.106
90	0	0	0	0	192	18.9	∞	0.106

[a] cf. ref. 4.

Finally, for conversion from one system to the other the relations

$$\left|\frac{d \cos \Phi}{d \cos \theta}\right| = \frac{\gamma^2}{4 \cos \Phi} (1 - \beta^2 \cos^2 \Phi)^2 \qquad (8)$$

and

$$\left|\frac{d \cos \Theta}{d \cos \theta}\right| = \frac{A \cos \theta + \gamma}{\{\sin^2 \theta + [A + \gamma \cos \theta]^2\}^{3/2}} \qquad (9)$$

are useful.

The targets chosen with the coincidence method were of thickness (CH_2) 0.290 g cm^{-2}, and (C) 0.338 g cm^{-2}, in the range of angles $25^\circ \leqslant \Phi \leqslant 50^\circ$. For small and large Φ thinner targets, of surface density less than 100 mg cm^{-2}, were used to reduce multiple scattering and allow the low energy particles to be counted in the crystals. It was found geometrically convenient to make the solid angle subtended by the proton crystal at angle Φ the defining one; this meant that the deuteron crystal at angle Θ had to be large enough and close enough to the target to count all deuterons from elastic d-p events in which the proton was counted in the other crystal. The values of distances b and c of the Φ and Θ crystals from the target (cf. Fig. 1) were so chosen as to satisfy this criterion, keep the angular resolution between 2° and 5°, and have the ratio of systematic to accidental coincidences as high as practicable.

When $\Phi \leqslant 15^\circ$ the deuterons have too short a range to be counted reliably. However, as illustrated in Table I, in this region of angles the proton has enough energy to have a range greater than that of the deuterons from the beam and from carbon. Moreover, the beam straggling was of the order of 1 g cm^{-2} of Al. Thus it was possible to single out the forward protons by using method D: a crystal was placed at angle Φ, and variable thicknesses of Al absorber were placed immediately in front of the crystal. The area of the absorber slabs was made much larger than that of the crystal face to provide a "poor" geometry. A thin Al wedge was centered over the crystal to equalize the energy of the particles entering it. The range of the particles depended on the target used (CH_2, C or Bl) since the targets had different stopping powers. The Al absorber was suitably adjusted to compensate for this effect. The targets were now of the order of 1 g cm^{-2}, since the hydrogen effect had to be separated from a large background coming directly from the collimator snout. The use of targets of this thickness was not expected to increase the straggling of the high energy elastic particles by more than 15 percent.
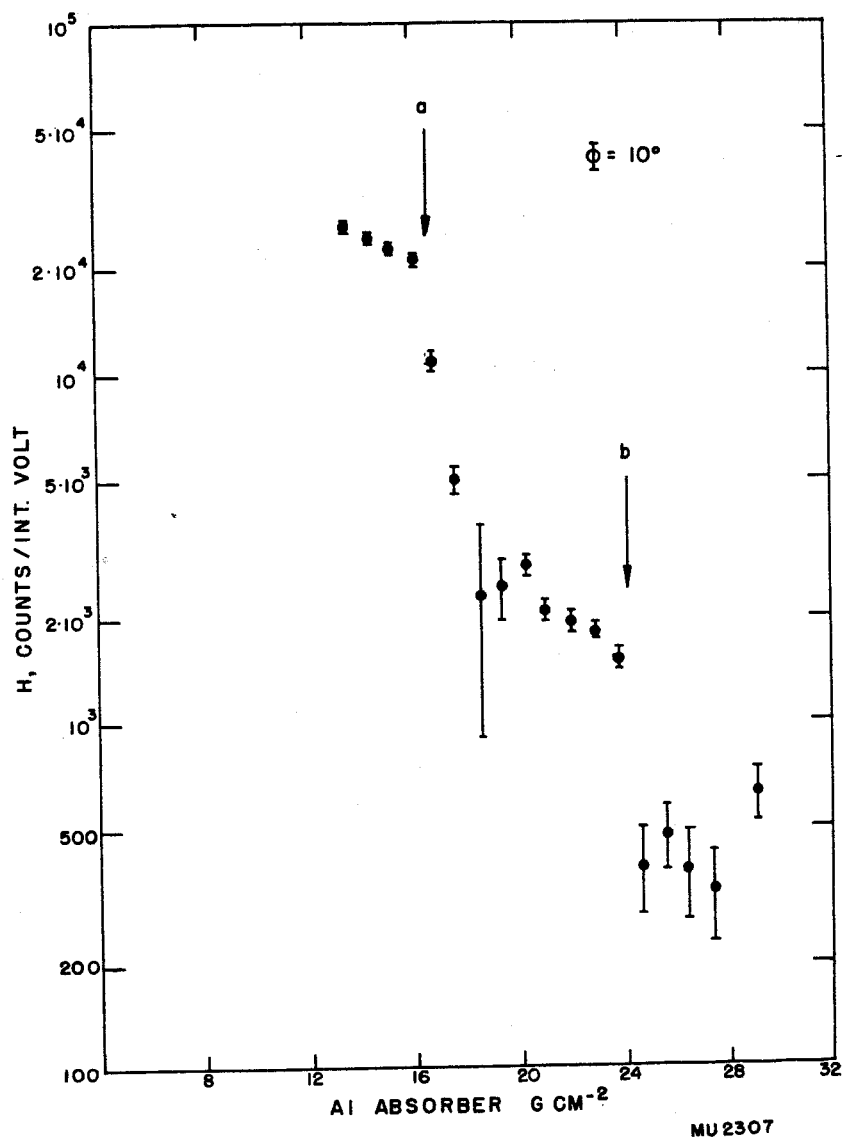
Fig. 2

A plot of $\underline{H}$, hydrogen counts per integrator volt at $\Phi = 10°$, versus absorber thickness is shown in Fig. 2. The various particles could be identified by their ranges.[4] The elastic protons were clearly distinguishable from a long range background and from shorter range particles, and were cut out by the expected amount of absorber (Arrow b, Fig. 2, and Table I). Similarly, the elastic deuterons of 181 Mev, corresponding to protons at $\Phi = 74°$ (Arrow a, Fig. 2) were also clearly identified. Finally, plots of $\underline{C}$ and $\underline{Bl}$ counts versus absorber had sharp breaks at values of absorber corresponding to the ranges of deuterons from carbon and from the beam, respectively. It was therefore possible, by this method, to obtain the elastic cross section for small and large center of mass angles θ for which the coincidence technique was unsuited. The relatively large background, which did not decrease appreciably with increasing absorber, was ascribed to events made by neutrons stripped[5] from high energy deuterons in the aluminum.

C. Sample Calculation.

1. Coincidence Method

Here we shall pick out a set of data taken with

$\Phi = 35°$, $\Theta = 29.2°$

Crystal at angle Φ: area = 9.88 cm^2

b = 92.5 cm, $\Delta\Omega = 1.155 \times 10^{-3}$ sterad

Crystal at angle Θ: area = 36 cm^2

c = 92.5 cm

Targets: CH_2: 0.290 g cm^{-2}

C: 0.338 g cm^{-2}

$\S$, the angle made by target plane with deuteron arm, = 25°

Integrating Condenser C_o: 1.021×10^{-7} f

Chamber Pressure: 78.4 cm Hg at 23° C

Chamber Multiplication μ: 1801

Effective Resolving Time τ: $(1.5 \pm 0.3) \times 10^{-5}$ sec. (cf. BC).

The data for one of several cycles of alternating CH_2, C, and Bl sequences are summarized in Table II.

TABLE II

Typical set of data for elastic d-p scattering at proton angle $\Phi = 35^\circ$ (Method C).

Target	Time sec.	Φ (Telesc. Coinc.)	Total Counts Θ	(Triple) Coinc.	Integrator Volts
CH_2	314	1989	26988	90	3.0
C	227	1098	16856	7	2.1
Bl	210	391	7030	2	2.0

From analysis described in BC, $z = 1.08 \pm 0.20$, and from Eq. (1), BC, $H = 26.5 \pm 3.5$

$t = \dfrac{0.200}{\sin 54.2^\circ}$, so from Eq. (5), BC,

$$N = 3.09 \times 10^{22} \text{ atoms cm}^{-2}.$$

From Eq. (6), BC, $n = 3.54 \times 10^8$ deuterons/I.V.

Eq. (4), BC, then yields $\sigma\ (\Phi = 35^\circ) = 2.10 \pm 0.28$ mb sterad^{-1}. To convert to the center of mass, we use the relation

$$\sigma\ (\theta) = \left| \frac{d \cos \Phi}{d \cos \theta} \right| \sigma\ (\Phi) \quad \text{where at } \Phi = 35^\circ,$$

$$\theta = 107.6^\circ, \quad \left| \frac{d \cos \Phi}{d \cos \theta} \right| = 0.297 \tag{10}$$

Hence $\sigma\ (\theta = 107.6^\circ) = (0.62 \pm 0.08) \times 10^{-27}$ cm^2 sterad^{-1}.

2. Single Count Method.

We shall choose $\Phi = 10^\circ$ or $\Theta = 10^\circ$, as illustrated in Fig. 2.

Crystal: area = 9.55 cm^2

distance from target: 100 cm

$\therefore \Delta\Omega = 9.55 \times 10^{-4}$ sterad.

Targets: CH_2: 0.991 g cm^{-2}

C: 1.284 g cm^{-2}

both oriented normal to the beam.

C_o: 0.99 × 10^{-6} f

Chamber pressure: 77.4 cm Hg at 22° C;

$$\mu = 1784$$

$$z = R = 0.661 \text{ (cf. Eq. (1) and text following, BC)}$$

The C target was equivalent in stopping power to 1.67 g cm^{-2} Al, the CH$_2$ target to 1.53 g cm^{-2} Al, so a slight extrapolation had to be made. The effect was obtained by taking the difference between the last point for which all the particles in question seemed to come in, and the background. The error assigned was the statistical error of the point compounded with that of the background.

TABLE III

Sample data for elastic d-p scattering at 10°, single count method, as a function of aluminum absorber in front of the detector. All data normalized to same integrated beam current.

Target	RANGE, g cm^{-2} Al			
	$(24.7 - 29.1)_{ave.}$	22.9	20.3	16.1
CH$_2$	5590 ± 35	7740 ± 70	11740 ± 130	81000 ± 500
C	6330 ± 35	7380 ± 100	11860 ± 220	83000 ± 700
Bl	2890 ± 40	3040 ± 100	3150 ± 100	14630 ± 350
H	440 ± 50	1830 ± 110	2800 ± 200	21200 ± 700

For $\Phi = 10^\circ$, H_p = (1830 ± 110) - (440 ± 50) = 1390 ± 120.

For $\Theta = 10^\circ$, H_d = (21200 ± 700) - (2800 ± 200) = 18400 ± 750.

$N = 8.58 \times 10^{22}$ atoms cm^{-2},

$n = 3.43 \times 10^9$ deuterons/volt.

$\sigma \ (\Phi = 10^\circ) = 4.95 \pm 0.43$ mb sterad^{-1};

From Table I, $\dfrac{d \cos \Phi}{d \cos \theta} = 0.234$ at $\Phi = 10^\circ$, $\theta = 159.2^\circ$.

In the center of mass system, therefore,

$$\sigma \ (\theta = 159.2) = (1.16 \pm 0.10) \cdot 10^{-27} \text{ cm}^2 \text{ sterad}^{-1}.$$

$\sigma \ (\Theta = 10^\circ) = 66.5 \pm 2.7$ mb sterad^{-1};

from Table I, $\dfrac{d \cos \Theta}{d \cos \theta} = 0.107$ at $\Theta = 10^\circ$, $\theta = 31.1^\circ$.

In the center of mass system, therefore,

$$\sigma \ (\theta = 31.1^\circ) = (7.0 \pm 0.3) \cdot 10^{-27} \text{ cm}^2 \text{ sterad}^{-1}.$$

D. Presentation of Data.

It should be mentioned that the elastic cross sections obtained with Method D are subject to some corrections. The protons observed at a certain angle Φ are attenuated by the nuclei in the absorber. A cross section $\sigma = \pi A^{2/3} r_o^2$, with $r_o = 1.4 \times 10^{-13}$ cm, was chosen to correct for this effect, and an error of 20 percent was applied to the correction. The number of deuterons observed at a given angle Θ had to be similarly corrected; another correction of + 5 percent had to be applied to compensate for stripping losses.[5] It is clear that, apart from systematic errors discussed in the next section, the elastic cross section obtained with all methods is an upper limit, inasmuch as some inelastic events may have been included. If one assumes a just inelastic d-p collision with one proton going forward at high energy and the other proton and neutron remaining close neighbors (say in the S state), the energetic proton would have of the order of only 3 Mev less energy than one scattered forward elastically. This effect may be sizable, especially for large θ, but no attempt has been made to correct for it.

The data, duly corrected, are summarized in Table IV. They have been averaged for a given angle over a given day's run, but results for the same angle obtained on a different day have been included separately. Values marked with asterisks were obtained with method D, all others with methods A-C. Figure 3 shows a plot of the results listed in Table IV, center of mass cross sections as ordinate, center of mass angle as abscissa. By passing a smooth curve through the weighted mean cross sections with a cut-off at $\theta = 10^o$ we found a total cross section from 10° to 180° in the center of mass of 34 ± 3 mb. The errors quoted in Fig. 3 are r.m.s. deviations due to counting statistics, absorber corrections and systematic uncertainties.

E. Errors.

The estimated errors discussed in some detail in this section refer mainly to the coincidence methods A, B, and C, however those of the first three paragraphs apply to all four methods.

Geometry: Alignment of the whole scattering table, 1°. Measurement of angles of counters with respect to the scattering table, 1/2 degree. The distance b defined in Fig. 1 was believed measured to 5 mm in 50 to 100 cm, so gave rise to solid angle uncertainties of about 2 percent. Target orientation was known to 1°, giving the effective target thickness to 1/2 percent to 1 percent. Crystal areas were all known to 2 percent. An error of 3 percent is attributed to uncertainty in interpretation of the bias curves of the counters.

TABLE IV

Summary of elastic d-p differential scattering cross sections
in the center of mass as a function of center of mass angle
θ. Figures of the last column include the systematic errors
of **Sec. E**.   Cross sections obtained with the "single count
method" are marked with an asterisk.

θ degrees	$\sigma(\theta)$ 10^{-27} cm^2/sterad	r.m.s. Counting Error 10^{-27} cm^2/sterad	$\overline{\sigma(\theta)}$ 10^{-27} cm^2/sterad	r.m.s. Total Error 10^{-27} cm^2/sterad
15.4	31.1*	3.2	31.1	5.1
31.1	8.9*	0.5	8.9	1.3
38.4	6.6	0.4		
	4.9	0.6		
	4.8	0.3	5.3	0.5
48.1	4.4	0.3		
	4.6	0.3		
	3.65*	0.17	4.0	0.4
57.8	2.14	0.07		
	2.54	0.11	2.33	0.21
67.6	1.22	0.05	1.22	0.10
77.5	1.16	0.06	1.16	0.10
81.5	0.89	0.05	0.89	0.08
87.5	0.70	0.03		
	0.77	0.08	0.71	0.06
97.5	0.59	0.04		
	0.73	0.05	0.64	0.05
107.6	0.61	0.03	0.61	0.05
117.8	0.52	0.08	0.52	0.09

TABLE IV

(Continued)

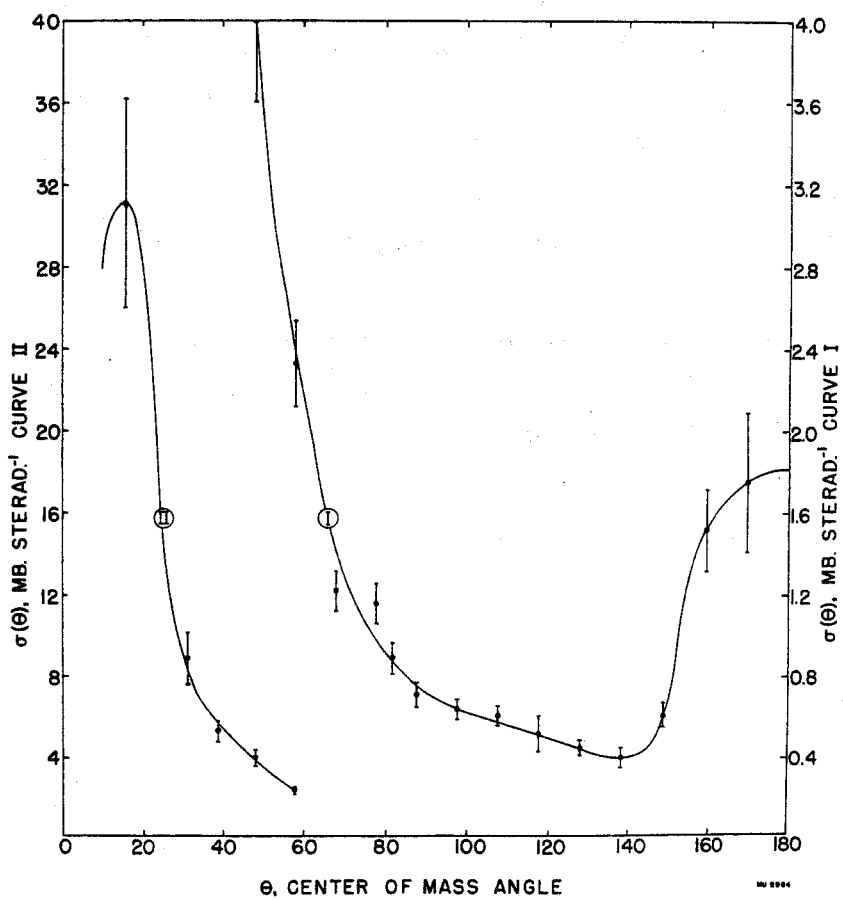| θ degrees	$\sigma\ (\theta)$ 10^{-27} $cm^2/sterad$	r.m.s. Counting Error 10^{-27} $cm^2/sterad$	$\overline{\sigma\ (\theta)}$ 10^{-27} $cm^2/sterad$	r.m.s. Total Error 10^{-27} $cm^2/sterad$
128.0	0.55	0.17		
	0.67	0.06		
	0.67	0.18		
	0.55	0.13		
	0.73	0.10		
	0.57	0.06		
	0.54	0.05		
	0.45	0.04	0.55	0.04
138.4	0.72	0.27		
	0.27	0.09		
	0.42	0.06		
	0.42	0.08	0.40	0.05
148.7	0.27	0.23		
	0.51	0.25		
	0.67	0.07		
	0.62	0.12		
	0.24	0.14		
	0.67*	0.07		
	0.61*	0.07	0.61	0.06
159.2	1.45	0.50		
	1.53*	0.13	1.52	0.20
169.5	1.75*	0.25	1.75	0.34

Fig. 3

Beam current measurement: The faraday cup calibration of Chamberlain, Segrè, and Wiegand[6] was thought accurate to 2 percent. Saturation of the argon-filled ionization chamber was guaranteed to 1 percent.

Targets: The hydrogen content of the polyethylene targets was known from analysis to 1 percent.

Multiple scattering: 2 percent error is estimated except where the angle Φ exceeded $60°$, in which case 5 percent was estimated. No appreciable loss is attributed to multiple scattering in the telescope of method C.

Finite counter resolving time: Counting rate losses amounted to no more than 2 percent at the highest counting rates allowed.

Carbon subtraction: Errors not greater than 2 percent, due mainly to duty cycle variations that might have escaped unnoticed.

Inelastic scattering: The possible inclusion of some inelastic d-p scattering events among those counted may have resulted in error of perhaps 3 percent.

We summarize by giving the systematic r.m.s. errors for the experiment. In the coincidence methods when θ was greater than $60°$, 7 percent. When θ was less than $60°$, the coincidence methods gave 9 percent error. Finally method D is believed accurate to 13 percent. Errors from counting statistics are to be combined with these values.

II COMPARISON WITH THEORY

A. General Considerations.

We shall try to use our experimental results on d-p scattering in order to gain additional knowledge about np and pp scattering. The theory of d-p scattering has been attacked by Wu and Ashkin,[7] Chew,[1,8,9,10] and Gluckstern and Bethe.[11]

In all previous work the Born or impulse approximation was used, and in some of it an attempt was made to identify certain terms in the d-p scattering amplitude with the n-p and p-p scattering amplitudes. In this connection it has usually been said that in calculating the d-p cross sections one is interested in the n-p and p-p cross sections obtained from experiments done with the same relative velocities. That is, one should be concerned with n-p and p-p differential scattering cross sections at 95 Mev when calculating the scattering of 190 Mev deuterons by stationary protons. The angles are correlated by the requirement that the magnitude of momentum transferred should be the same in all cases.

This is quite true at small angles of scattering, as is shown by both impulse approximation and Born approximation. However, it seems worthwhile to comment that as one examines larger angle elastic d-p scattering, one should compare with n-p and p-p scattering at a higher energy.

Our argument is based on the Born approximation, and is believed to apply equally to the impulse approximation inasmuch as one can easily construct hypothetical parameters for n-p and p-p interactions such that both Born approximation and impulse approximation are guaranteed to be valid.

We write the amplitude for elastic d-p scattering in the form used by Chew,[8] employing for the n-p interaction a potential which is partly ordinary force and partly exchange force. (The p-p interaction may be treated formally the same way.) We obtain from the ordinary force the integral Chew has called I_1, and from the exchange force the integral I_2. The factor $S^{1/2}$ can be taken from I_1 immediately. (S is the "sticking factor" of Chew.) The same factor can be taken from I_2 if the suitable approximation is made, that the potentials used are more singular than the deuteron wave function. The remaining integrals are

$$I_1/S^{1/2} = \int d\underline{x}\, e^{-i(\underline{k}_f - \underline{k}_o)\cdot \underline{x}} V_{ord}(\underline{x})$$

and
$$I_2/S^{1/2} \cong \int d\underline{x}\, e^{-\frac{3}{4}i(\underline{k}_f + \underline{k}_o)\cdot \underline{x}} V_{exch}(\underline{x})$$

(11)

where $\underline{k}_f$ and $\underline{k}_o$ are final and initial momenta in the c.m. system (divided by $\hbar$). The corresponding expressions for free n-p scattering are

$$I_1' = \int d\underline{x}\, e^{-i(\underline{k}_f'' - \underline{k}_o')\cdot \underline{x}}\, V_{ord}(x)$$

$$(12)$$

and $$I_2' = \int d\underline{x}\, e^{-i(\underline{k}_f' + \underline{k}_o')\cdot \underline{x}}\, V_{exch}(x)$$

where $\underline{k}_f'$ and $\underline{k}_o'$ have the corresponding meanings in the c.m. system for neutron and proton. In order that $I_1/S^{1/2} = I_1'$ and $I_2/S^{1/2} = I_2'$ (so that n-p scattering amplitudes may be correctly used in the d-p expression) the following relations must hold:

$$\left| \underline{k}_f - \underline{k}_o \right| = \left| \underline{k}_f' - \underline{k}_o' \right| ,$$

$$\frac{3}{4}\left| \underline{k}_f + \underline{k}_o \right| = \left| \underline{k}_f' + \underline{k}_o' \right| .$$

$$(13)$$

For a given energy and angle of d-p scattering these relations determine the energy and angle of the n-p scattering such that the scattering amplitudes appear directly in the d-p expressions. We include in Table V the values of energy (laboratory system) and angle (c.m. system) for n-p scattering corresponding to various angles (c.m. system) for the present case of 192 Mev deuterons scattered by protons.

TABLE V

Center of mass angle θ' and laboratory energy E' to be used in the nucleon-nucleon scattering amplitudes associated with d-p scattering at center of mass angle θ.

θ c.m. degrees	θ' c.m. degrees	E' lab. syst., Mev
$0°$	$0°$	96
$20°$	$26°$	98
$40°$	$52°$	103
$60°$	$74°$	115
$80°$	$95°$	127

B. Analysis Without Tensor Forces.

In this section we wish to follow the very elegant method used by Chew,[1] and to point out a few examples which may be used as guides in further work. As will perhaps be evident to some readers, we propose to take the results of Chew more seriously than does he. It is our hope that in the near future more explicit analyses of the errors in the impulse approximation, as applied to this problem, may be available.

We write Chew's result in the following form:

$$\frac{9}{16} \frac{\sigma_{dp}(\theta)}{S(K)} = \left| r^o_{np} + r^o_{pp} \right|^2 + \frac{2}{3} \left| r^1_{np} + r^1_{pp} \right|^2 \tag{14}$$

where $\underline{K} = \underline{k}_f - \underline{k}_o$, S (K) is the sticking factor defined by Chew (with the Hulthen wave function representing the bound state of the deuteron), r^o (frequently called the "amplitude for scattering without spin flip") is defined in terms of triplet and singlet scattering amplitudes (r^t and r^s) as follows:

$$r^o = \frac{3}{4} r^t + \frac{1}{4} r^s , \tag{15}$$

and r^1 (the "amplitude for scattering with spin flip") is

$$r^1 = \frac{\sqrt{3}}{4} (r^t - r^s) . \tag{16}$$

The complex scattering amplitudes so defined have the very convenient properties

$$\sigma_{np}(\theta) = \left| r^o_{np} \right|^2 + \left| r^1_{np} \right|^2 , \tag{17}$$

and the identical relation for p-p scattering.

If, then, the break-up of the n-p and p-p scattering into scattering with and without spin flip were known, the elastic d-p cross section could be reliably predicted, at least at fairly small angles where the approximations used are good. It is interesting that the spin flip term enters in Eq. (14) with such a large coefficient as 2/3, which corresponds to the fact that spin flip phenomena most frequently leave the deuteron in a triplet state, due to the large statistical weight.

We take the n-p and p-p cross sections as known,[6,12,13,14,15] even though we have to interpolate somewhat between observations to cover the energy

region 95 to 130 Mev. However, the analysis into scattering amplitudes with and without spin flip is not known, and we wish to test several assumptions.

The simplest assumption is that both n-p and p-p scattering are completely without spin flip and there is no great phase difference between the scattering amplitudes. This leads to the largest possible elastic d-p scattering, and the result is plotted in Fig. 4, Curve A. This cross section is much larger than that observed, Curve D, which is shown in the same figure.

The next, and more reasonable, assumption would be that n-p and p-p forces are identical (can be derived from the same potential) and that only even states are present in the scattering (Serber potential).[17] With these assumptions the Pauli principle dictates that the p-p scattering be all singlet scattering, and the p-p scattering may be used to deduce the separation of n-p scattering into singlet and triplet states. With the further assumption that the phase differences between singlet and triplet amplitudes are not large, the resulting d-p scattering is indicated also in Fig. 4, Curve B. Again the calculated result is somewhat too large.

One gets results closer to those observed by assuming that n-p scattering involves no spin flip, and that p-p scattering is all with spin flip. However, this proposal is not a reasonable one from the viewpoint of other work. It does not agree at all with any of the potentials calculated for n-p and p-p scattering, and it does not allow for charge independence of nuclear forces. Curve C shows this result quite close to that observed.

We have found it helpful to visualize r^o and r^1 as the two components of a vector in a two-dimensional space (i.e., one vector for n-p, and another for p-p scattering), and to say that this analysis is summarized by the statement that the amplitude vectors for n-p and p-p scattering must be approximately perpendicular to each other to allow agreement between theory and experiment.

C. Analysis With Tensor Forces.

We must now write Chew's result in the more general form

$$\frac{9}{16} \frac{\sigma_{dp}(\theta)}{S(K)} = \left| r^o{}_{np} + r^o{}_{pp} \right|^2 + \frac{2}{3} \left| \vec{r}_{np} + \vec{r}_{pp} \right|^2, \tag{18}$$

where $\vec{r}_{np}$ and $\vec{r}_{pp}$ have been written as vectors to indicate that there are three component amplitudes r^1 to r^3 involved. Thus four amplitudes for n-p and p-p are now needed to deduce the cross section. We shall show below how these are found. Again we have
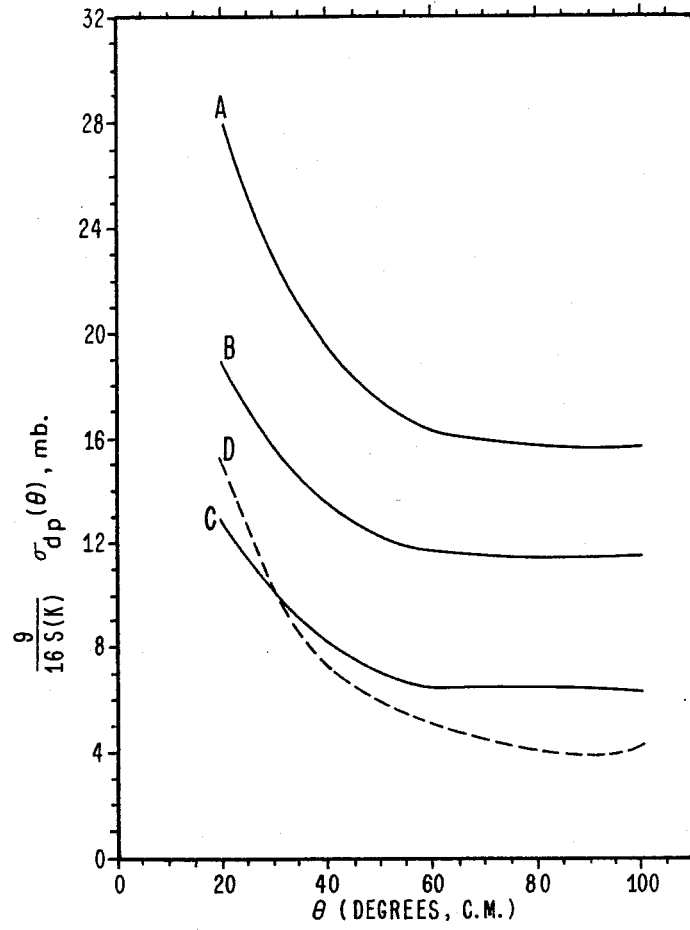
MU 5589

Fig. 4

$$\sigma_{np}(\theta) = \sum_{i=0}^{3} |r^i{}_{np}|^2 \tag{19}$$

and a similar relation for the p-p cross section.

Once a potential has been assumed, the breakup of n-p and p-p scattering into r^o, r^1, r^2 and r^3 can be found. The d-p cross section can then be written and compared with experimental values. A suitable program would therefore be to take a great variety of potentials that lead to correct nucleon-nucleon scattering cross sections, calculate d-p scattering from them by using the nucleon-nucleon phase shifts, and compare with experiment. One would thereby hope to be able to eliminate a great number of potentials as unsuitable.

Unfortunately, the number of potentials that have so far succeeded in describing nucleon-nucleon scattering experiments adequately is small - we shall consider four - and the task of computing and using partial phase shifts is beyond our scope. We have therefore, with one exception, limited ourselves to the Born approximation in calculating the two sets of four scattering amplitudes. Instead of comparing the d-p cross section calculated from these directly with experiment, we compare it with the n-p and p-p cross sections derived from the same scattering amplitudes.

We then make the plausible postulate that the relation found to hold between experimental n-p, p-p and d-p differential scattering cross sections should exist, to good approximation, between the same cross sections as calculated from scattering amplitudes derived in Born approximation, if the potential assumed is to have validity; it is felt that this relation should be maintained to good approximation even though the Born approximation does not render the cross sections very faithfully at the energies involved here. The relation found to hold between measured cross sections was that (apart from the sticking factor) the n-p and p-p waves did not strongly interfere in d-p scattering; i.e., the amplitude vectors for n-p and p-p scattering were roughly orthogonal. We postulate that this orthogonality must still hold when the components of the vectors (now four-fectors due to inclusion of tensor forces) are calculated in Born approximation. Accordingly we are interested in comparing the ratios $\dfrac{\sigma_{dp}}{\sigma_{np} + \sigma_{pp}}$ for experiment and for various calculated potentials. We shall limit ourselves to scattering angles less than 90° in the center of mass, as the expression (18) breaks down at large angles.

We now write, in the usual way,

$$\psi \chi \rightarrow e^{ik_o z} \chi_{inc} + \frac{e^{ik_o r}}{r} S \chi_{inc} \tag{20}$$

where ψ denotes the asymptotic form of the total wave function, χ its spin part, and k_o is the propagation number in the center of mass. S will be called the scattering matrix. When evaluated in Born approximation, it will be denoted by $^B S$. Our procedure will be to find the 4 x 4 matrix $^B S$ for nucleon-nucleon scattering derived from a given potential and expressed in a suitably simple reference frame, to identify r^o to r^3, and therefrom to find the nucleon-nucleon and d-p cross sections. In this process the 6 x 6 scattering matrix for d-p scattering can be derived and Chew's expression checked. Finally the ratios $\dfrac{\sigma_{dp}}{\sigma_{np} + \sigma_{pp}}$ will be compared with those obtained from experimental values.

We shall derive the nucleon-nucleon cross section for identical particles labelled 1 and 2. Extension to non-identical particles is obvious. We are given a potential $U\ (\underline{r},\ \sigma)\ \dfrac{\hbar^2}{2m}$ and have, for the scattering amplitude in Born approximation,

$$f - f' = f\ (\theta,\ \phi,\ \chi_{12}) - f\ (\pi - \theta,\ \pi + \phi,\ \chi_{21}) = {}^B S \chi_{inc}^{12} - {}^B S' \chi_{inc}^{21} \qquad (21)$$

where

$$^B S = \frac{1}{4\pi} \int U\ (\vec{r},\ \sigma)\ e^{i(\underline{k}_o - \underline{k}_f)\ \cdot\ \underline{r}}\ d\underline{r}\ , \qquad (22)$$

and

$$^B S' = \frac{1}{4\pi} \int U\ (\underline{r},\ \sigma)\ e^{-i(\underline{k}_o + \underline{k}_f)\ \cdot\ \underline{r}}\ d\underline{r}. \qquad (23)$$

The cross section is obtained by squaring $f - f'$ and averaging over all initial spin states. We now specify

$$U^t\ (\underline{r},\ \sigma) = \frac{2m}{\hbar^2}\ \left[J_c\ (r) + J_t\ (r)\ S^{12} \right] \qquad (24)$$

for the triplet interaction, with

$$S^{12} = 3\ \frac{(\underline{\sigma}_1 \cdot \underline{r})(\underline{\sigma}_2 \cdot \underline{r})}{r^2} - \underline{\sigma}_1 \cdot \underline{\sigma}_2, \text{ and} \qquad (25)$$

$$U^s\ (\underline{r},\ \sigma) = \frac{2m}{\hbar^2}\ J'_c\ (r) \qquad (26)$$

for the singlet interaction. Substitution yields

$$^B S = F\ (\theta) \begin{pmatrix} 1 & 0 & 0 & 0 \\ 0 & 1 & 0 & 0 \\ 0 & 0 & 1 & 0 \\ 0 & 0 & 0 & 0 \end{pmatrix} + F'\ (\theta) \begin{pmatrix} 0 & 0 & 0 & 0 \\ 0 & 0 & 0 & 0 \\ 0 & 0 & 0 & 0 \\ 0 & 0 & 0 & 1 \end{pmatrix} + C\ (\theta)\ \left\| T\ (\theta,\ \phi) \right\| \qquad (27)$$

and

$$B_{S'} = F(\pi - \theta) \begin{pmatrix} 1 & 0 & 0 & 0 \\ 0 & 1 & 0 & 0 \\ 0 & 0 & 1 & 0 \\ 0 & 0 & 0 & 0 \end{pmatrix} - F'(\pi - \theta) \begin{pmatrix} 0 & 0 & 0 & 0 \\ 0 & 0 & 0 & 0 \\ 0 & 0 & 0 & 0 \\ 0 & 0 & 0 & 1 \end{pmatrix} + C(\pi - \theta) \,||\, \tau(\pi - \theta, \pi + \phi) \,|| \qquad (28)$$

where

$$F(\theta) = \frac{2m}{\hbar^2} \int_0^\infty J_c(r) \frac{\sin Kr}{Kr} r^2 \, dr, \qquad (29)$$

$$F'(\theta) = \frac{2m}{\hbar^2} \int_0^\infty J_c'(r) \frac{\sin Kr}{Kr} r^2 \, dr, \qquad (30)$$

and

$$C(\theta) \,||\, \tau(\theta, \phi) \,|| = \frac{m}{2\pi \hbar^2} \int J_t(r) S^{12} e^{i(\underline{k}_o - \underline{k}_f) \cdot \underline{r}} \, d\underline{r}. \qquad (31)$$

where

$$C(\theta) = \frac{m}{\hbar^2} \int_0^\infty J_t(r) \left[\frac{6 \sin Kr}{K^3 r^3} - \frac{6 \cos Kr}{K^2 r^2} - \frac{2 \sin Kr}{Kr} \right] r^2 \, dr. \qquad (32)$$

The value of the 4 x 4 matrix $||\, \tau \,||$ depends on the polar axis chosen for the representation. As pointed out by Ashkin and Wu[16], we can choose the polar axis along $\underline{K} = \underline{k}_o - \underline{k}_f$, and this procedure yields

$$||\, \tau(\theta, \phi) \,|| = \underline{\sigma}_1 \cdot \underline{\sigma}_2 - 3\sigma_{1K} \sigma_{2K} \qquad (33)$$

where the σ are the   Pauli spin matrices. In particular, we can make K coincide with the axis of spin quantization. This will make $||\, \tau(\theta, \phi) \,||$ diagonal, but not $||\, \tau(\pi - \theta, \pi + \phi) \,||$. It is easy to see that since

$$||\, \tau' \,|| = ||\, \tau(\pi - \theta, \pi + \phi) \,|| = \underline{\sigma}_1 \cdot \underline{\sigma}_2 - 3\sigma_{1K'} \sigma_{2K'},$$

and $\underline{K}' \equiv -(\underline{k}_o + \underline{k}_f)$ is perpendicular to $\underline{K}$, $||\, \tau \,||$ and $||\, \tau' \,||$ commute, and can be diagonalized simultaneously. It will be convenient to do so. The result is

$$||\, \tau \,|| = \begin{pmatrix} -2 & 0 & 0 & 0 \\ 0 & 4 & 0 & 0 \\ 0 & 0 & -2 & 0 \\ 0 & 0 & 0 & 0 \end{pmatrix}, \qquad ||\, \tau' \,|| = \begin{pmatrix} -2 & 0 & 0 & 0 \\ 0 & -2 & 0 & 0 \\ 0 & 0 & 4 & 0 \\ 0 & 0 & 0 & 0 \end{pmatrix} \qquad (34)$$

where the rows and columns are labelled by basis vectors

$$\xi_1 = \frac{1}{\sqrt{2}} (\alpha_1 \alpha_2 - \beta_1 \beta_2), \qquad \xi_2 = \frac{1}{\sqrt{2}} (\alpha_1 \beta_2 + \beta_1 \alpha_2), \qquad \xi_3 = \frac{1}{\sqrt{2}} (\alpha_1 \alpha_2 + \beta_1 \beta_2); \qquad (35)$$

$$\xi_4 = \frac{1}{\sqrt{2}} (\alpha_1 \beta_2 - \beta_1 \alpha_2),$$

that is, in choosing a z-axis different than the K-axis we have mixed the basis vectors for spin components 1 and - 1 along the K axis, leaving the components 0 in triplet and singlet unaltered.

We can now write down the result

$$f - f' =$$
$$\chi_{inc}^{12} \begin{pmatrix} F(\theta) - F(\pi-\theta) - 2\left[C(\theta) - C(\pi-\theta)\right] & 0 & 0 & 0 \\ 0 & F(\theta) - F(\pi-\theta) + 4C(\theta) + 2C(\pi-\theta) & 0 & 0 \\ 0 & 0 & F(\theta) - F(\pi-\theta) - 2C(\theta) - 4C(\pi-\theta) & 0 \\ 0 & 0 & 0 & F'(\theta) + F'(\pi - \theta) \end{pmatrix} \qquad (36)$$

and the p-p cross section is at once obtained by squaring and averaging over initial spins, which yields one-fourth the sum of the squares of the matrix elements. In order to derive the d-p cross section, we would like now to find r^0 to r^3. In this we are guided by our definitions for r^0 and r^1 with central forces only. Call $\phi_1 \cdots \phi_4$ the four diagonal elements of the preceding matrix. We are lead to write

$$r^0 = \frac{1}{4} (\phi_1 + \phi_2 + \phi_3 + \phi_4),$$

$$r^1 = \frac{1}{4\sqrt{3}} (\phi_1 + \phi_2 + \phi_3 - 3\phi_4). \qquad (37)$$

Note that since $\| \tau \|$ and $\| \tau' \|$ have zero trace, tensor forces do not enter r^0 and r^1. r^2 and r^3 must now be defined in such a way that condition (19) is satisfied, i.e.

$$\sigma_{pp} = \sum_{i=0}^{3} |r_{pp}^i|^2 = \frac{1}{4} \sum_{j=1}^{4} |\phi_j|^2 \qquad (38)$$

This leaves two possibilities, of which we choose the one that yields the greater symmetry in $C(\theta)$ and $C(\pi - \theta)$:

$$r_2 = \frac{1}{2\sqrt{6}} (2\phi_1 - \phi_2 - \phi_3),$$

$$r_3 = \frac{1}{2\sqrt{2}} (\phi_3 - \phi_2).$$

(39)

Note that neither r^2 nor r^3 contain central force terms.

Having found the amplitudes for n-p and p-p scattering in various two-particle spin states, we need merely expand the six possible total spin functions of the d-p system (four quartet and two doublet states, the latter symmetric in spins of the particles in the deuteron) $\chi_{1....6}$ in terms of the two-particle functions $\xi_{1..4}$ (35), multiply by each of the $\chi_{1....6}$ in turn and remember that the amplitude for scattering from a state ξ_i to a state ξ_j is $\phi_i \delta_{ij}$. We thus obtain the 6 x 6 Born scattering matrix for deuteron-proton scattering. One-sixth the sum of squares of its elements gives the d-p cross section (apart from a factor $\frac{16}{9} S(K)$) in terms of the ϕ_i. This expression can then be expanded in terms of the r^i. Chew's expression is the result, and since we know the r^i for a given potential, $\sigma_{dp}(\theta)$ can be found in Born approximation.

It may be instructive to try to evaluate $\sigma_{dp}(\theta)$ to a somewhat higher approximation. In one of the cases (hard core, fourth potential, see below) the singlet and triplet phase shifts for definite energies were actually available. The scattering matrices for nucleon-nucleon scattering were therefore computed "exactly" in a convenient reference frame*, and were afterwards transformed to the reference frame in which $^B S$ and $^B S'$ had been found to be diagonal. In this frame it was found that all matrix elements of the exact scattering matrix were zero except the four diagonal ones and the (23) and (32) elements, with the latter the negative of the former. Thus five parameters were now necessary to describe the nucleon-nucleon cross sections and hence the d-p cross section. The latter would have to be calculated in the same manner as before, with Chew's result no longer valid. The d-p cross section could at best be calculated in impulse approximation from exact nucleon-nucleon scattering amplitudes. It was therefore felt that inasmuch as the off-diagonal elements were rather small for the p-p case and altogether negligible for n-p, they could be omitted and the previous machinery used for calculating the d-p scattering cross section. That this

---

*The energy dependence of the nucleon-nucleon amplitudes entering the d-p amplitude (cf. Table V) was here ignored: the energies available were 90 Mev for n-p, 129 Mev for p-p.

method of calculating nucleon-nucleon cross sections is far superior to the Born approximation is shown by the comparisons made in Table VII.

The four different potentials used in the calculation are presented in Table VI.

The CH - CN potentials are charge dependent. They are characterized by Serber forces (even states only) in n-p and by a singular tensor force in odd p-p triplet states. They were proposed by Christian, Hart and Noyes[17,18] working under Serber.

The CNS potential is charge independent, and leads only to even states except for a singular tensor force in both n-p and p-p odd triplet states. It was adapted by Don Swanson from the CN potential.

The JS potential is characterized by a hard repulsive core in singlet states. It is charge independent, and was first proposed by Jastrow[19] and adapted by Swanson.

The JCH - JCN potentials are charge dependent and resemble the CH - CN potentials except that a hard core has been introduced in both singlet and triplet. They are modifications of a potential proposed by Jastrow.[19]

The Born scattering (real) amplitudes for the various potentials and the triplet (complex) exact amplitudes for the JCH - JCN potentials were provided by Don Swanson, the singlet phase shifts for the hard core potentials by R. Jastrow. Both attractive and repulsive singular tensor forces were tried in the first two potentials, only repulsive ones in the last two.

The results of the calculations are given in Table VII. It must be remembered that the n-p cross sections given are energy and angle dependent (See Table V), with the exception indicated in the footnote. A compromise value of 5 mb[6,13,15] was taken for the p-p cross section for all angles and energies.

It is clear that our conclusions derived from Table VII depend on our confidence in the impulse approximation. Deviations of the order of 10 or 20 percent from experiment certainly are not great enough to disqualify a potential.

We can say that both charge dependent potentials, CN - CH and JCH - JCN, are admissible. The charge-independent potential CNS should perhaps be ruled out, whereas JS provides good agreement. Thus it appears that charge independent potentials satisfying the experimental results of n-p, p-p and d-p scattering can be found; and that Jastrow's hard core is so far compatible with experience.

TABLE VI

This table describes the potentials used in the present calculations: CH = Christian and Hart, CN = Christian and Noyes, CNS = Christian, Noyes, and Swanson, JS = Jastrow and Swanson. IND = Charge Independent, B = Born Approximation, δ = Phase Shifts. Potentials in Mev. P is the space permutation operator, and S^{12} is the tensor operator defined in Eq. (25). Parameters, in 10^{-13} cm, are: $r_o = 1.35$, $r_1 = 2.615$, $r_2 = 1.6$, $r_3 = 0.60$, $r_4 = 0.40$, $r_5 = 0.48$, $r_6 = 0.24$.

Nucleon Pair	Potential	Singlet	Triplet	Method of Calculation Singlet	Method of Calculation Triplet
np	CH	$-35.3 \frac{1+P}{2} \frac{r_o}{r} e^{-\frac{r}{r_o}}$	$-25.3 \frac{1+P}{2} \frac{r_o}{r} e^{-\frac{r}{r_o}} - 48.3 (0.37 + 0.63P) \frac{r_o}{r} e^{-\frac{r}{r_o}} S^{12}$	B	B
pp	CN	$-13.273 \frac{1+P}{2}$, $r < r_1$; 0, $r > r_1$	$-25.3 \frac{1+P}{2} \frac{r_o}{r} e^{-\frac{r}{r_o}} - 48.3 \frac{1+P}{2} \frac{r}{r} e^{-\frac{r}{r_o}} S^{12} \pm 15.25 (\frac{1-P}{2}) (\frac{r_2}{r})^2 e^{-\frac{r}{r_2}} S^{12}$	B	B
IND.	CNS	$-13.273 \frac{1+P}{2}$, $r < r_1$; 0 $r > r_1$	$-25.3 \frac{1+P}{2} \frac{r_o}{r} e^{-\frac{r}{r_o}} - 48.3 \frac{1+P}{2} \frac{r_o}{r} e^{-\frac{r}{r_o}} S^{12} \pm 15.25 \frac{1-P}{2} (\frac{r_2}{r})^2 e^{-\frac{r}{r_2}} S^{12}$	B	B
IND.	JS	∞, $r < r_3$; $-375 \frac{1+P}{2} e^{-\frac{r-r_3}{r_4}}$, $r > r_3$	$-25.3 \frac{1+P}{2} \frac{r_o}{r} e^{-\frac{r}{r_o}} - 48.3 \frac{1+P}{2} \frac{r}{r_o} e^{-\frac{r}{r_o}} S^{12} + 15.25 \frac{1-P}{2} (\frac{r_2}{r})^2 e^{-\frac{r}{r_2}} S^{12}$	δ	B
np	JCH	∞, $r < r_3$; $-375 \frac{1+P}{2} e^{-\frac{r-r_3}{r_4}}$, $r > r_3$	$-25.3 \frac{1+P}{2} \frac{r_o}{r} e^{-\frac{r}{r_o}} - 48.3 \frac{1+P}{2} \frac{r_o}{r} e^{-\frac{r}{r_o}} S^{12}$	δ	δ
pp	JCN	∞, $r < r_3$; $-375 \frac{1+P}{2} e^{-\frac{r-r_3}{r_4}}$, $r > r_3$; ∞, $r < r_6$; $15.25 (\frac{r_2}{r_5})^2 e^{-\frac{r_5}{r_2}} \frac{1-P}{2} S^{12}$, $r_6 < r < r_5$; $+ 15.25 (\frac{r_2}{r})^2 e^{-\frac{r}{r_2}} \frac{1-P}{2} S^{12}$, $r > r_5$		δ	δ

TABLE VII

This table presents a summary of the calculations. Column 1 lists the d-p center of mass scattering angle θ. Columns 2-5 give the experimental pp, np, and d-p cross sections used at a given θ, and the ratio $\Delta = \sigma_{dp}/(\sigma_{np} + \sigma_{pp})$. The remaining columns list pp, np and dp cross sections calculated from the potentials heading the columns and described in Table VI. The letters in parenthesis give the approximations to which the nucleon-nucleon amplitudes were calculated in singlet and triplet, respectively. B = Born approximation, Σ = phase shifts. The approximation involved in the JCN - JCH calculation consisted in omitting the off-diagonal elements in the scattering matrices. All cross sections are in 10^{-27} cm² sterad⁻¹, and dp cross sections have been multiplied by $9/[16 \times S(K)]$.

θ_dp	Experimental				CN - CH (BB)		rep. tensor		att. tensor		CNS (BB)		repulsive tensor		attractive tensor			JS (ΣB)				JCH - JCN (Σ Σ)					
																						exact		approximate			
	σ_pp	σ_np	σ_dp	Δ	σ_pp	σ_np	σ_dp	Δ	σ_dp	Δ	σ_pp	σ_np	σ_dp	Δ	σ_np	σ_dp	Δ	σ_pp	σ_np	σ_dp	Δ	σ_pp'	σ_np'	σ_pp	σ_np	σ_dp	Δ
20°	5.0	9.5	15	1.03	8.4	4.9	16	1.16	14	1.06	8.4	5.4	18	1.31	5.6	19	1.32	3.9	3.7	7.0	0.92	4.7	12	4.5	12	18	1.09
40°	5.0	4.8	7.2	0.73	5.7	3.0	7.5	0.86	7.8	0.90	5.7	3.1	8.9	1.01	5.8	14	1.23	4.3	3.1	4.1	0.55	5.3	8.1	4.6	8.1	10	0.79
60°	5.0	3.4	5.4	0.64	5.0	2.7	6.4	0.83	4.9	0.64	5.0	3.0	7.7	0.96	4.6	11	1.14	4.9	2.7	4.4	0.58	5.5	5.1	4.6	5.1	7.0	0.72
80°	5.0	3.1	3.9	0.48	5.0	3.0	7.6	0.95	3.4	0.43	5.0	3.9	9.7	1.09	3.4	8.7	1.04	5.0	2.3	5.2	0.71	5.6	4.4	4.6	4.4	7.2	0.80

MU-5535

D. Conclusions.

These results indicate that the effect of tensor forces must be considered if even qualitative agreement with the elastic d-p scattering experiments is to be obtained. The argument used is that the otherwise most reasonable central force models of nucleon-nucleon interaction lead to prediction of more elastic d-p scattering than is observed. Since tensor forces have been extensively considered in nucleon-nucleon interaction, this result is perhaps not unexpected.

Unfortunately, the d-p scattering seems to differentiate rather poorly between the various models having significant contributions from tensor forces. In fact all of the models that have included tensor forces fit much better than any reasonable central force approximation. With some uncertainty, the CNS potential might be ruled out.

At the time this work was started there was less indication than there is at the present time of the charge independence of nuclear forces. It still seems appropriate, however, to include the results for some models which are not charge independent, most of which explain the present results quite well. Of the charge independent models, that of Jastrow as modified by Swanson (JS) is favored. How strongly it is favored depends to a large extent on how much confidence one has in the approximations used. The reader is referred to Table VII in which theory and experiment are compared on the basis of the quantity Δ.

Some of these conclusions have been brought out by Horie, Tamura, and Yoshida,[20] who have compared with the same experimental data presented here.

The suggestion is made that in a refined analysis of the d-p scattering at one energy, the data must be compared with nucleon-nucleon scattering measurements made at a variety of energies. The proposed energies and angles are indicated in Table V.

No attempt has been made in the present work to analyze the data in the region of 180 degrees in the c.m. system (the "pick-up" region).

ACKNOWLEDGMENTS

REFERENCES

1. G. F. Chew, Phys. Rev. 84, 1057 (1951).

2. A. L. Bloom and Owen Chamberlain, UCRL-2237, Phys. Rev. ___, hereafter referred to as BC.

3. C. Wiegand, Rev. Sci. Inst. 21, 975 (1950).

4. W. Aron, B. Hoffman and F. Williams, Range-Energy Curves, AECU-663 (UCRL-121, 2nd rev.), unpublished.

5. Robert Serber, Phys. Rev. 72, 1008 (1947).

6. O. Chamberlain, E. Segrè, and C. Wiegand, Phys. Rev. 83, 923 (1951).

7. Ta-You Wu and J. Ashkin, Phys. Rev. 73, 986 (1948).

8. G. F. Chew, Phys. Rev. 74, 809 (1948).

9. G. F. Chew, Phys. Rev. 80, 196 (1950).

10. G. F. Chew, Phys. Rev. 84, 710 (1951).

11. R. L. Gluckstern and H. A. Bethe, Phys. Rev. 81, 761 (1951).

12. J. Hadley, E. Kelly, C. E. Leith, E. Segrè, C. Wiegand, and H. York, Phys. Rev. 75, 351 (1949).

13. R. Birge, U. Kruse and N. Ramsey, Phys. Rev. 83, 274 (1951).

14. C. L. Oxley and R. D. Schamberger, Phys. Rev. 85, 416 (1952).

15. J. M. Cassels, G. H. Stafford and T. G. Pickavance, Nature 168, 468 (1951).

16. J. Ashkin and Ta-You Wu, Phys. Rev. 73, 973 (1948).

17. R. S. Christian and E. W. Hart, Phys. Rev. 77, 441 (1950).

18. R. S. Christian and H. P. Noyes, Phys. Rev. 79, 85 (1950).

19. Robert Jastrow, Phys. Rev. 81, 165 (1951).

20. H. Horie, T. Tamura and S. Yoshida, Prog. Theor. Phys. 8, 341 (1952).

FIGURE CAPTIONS

Fig. 1   Velocity diagram of a deuteron colliding with a target proton in the laboratory system; the distances $\underline{b}$ and $\underline{c}$ of the proton crystal and deuteron crystal from the target are shown, and angles $\underline{\Phi}, \Theta$ and δ of the text are defined.

Fig. 2   Hydrogen counts per unit beam charge as a function of Al absorber in front of the crystal (method D). Arrows $\underline{a}$ and $\underline{b}$ give the absorber, 16.7 g/cm^2 and 24.2 g/cm^2, at which, respectively, half the elastic deuterons (corresponding to $\underline{\Phi} = 73.8^{o}$) and protons ($\underline{\Phi} = 10^{o}$) are counted. Calculated ranges are 16.8 g/cm^2 and 24.0 g/cm^2, respectively.

Fig. 3   Averaged differential elastic cross sections in the center of mass, with their total errors. The curve was used to find the total cross section between 10° and 180°, 34 ± 3 mb.

Fig. 4   Plot of $9/(16\ S\ (K))$ times the d-p cross section in mb as a function of center of mass angle θ under various assumptions, central forces only.

        A.   n-p and p-p all non-spin flip.

        B.   Serber potential.[17]

        C.   n-p non-spin flip, p-p all spin flip.

        D.   Experimental values.